Performance limiting effects in *X*-band accelerators

Faya Wang, Chris Adolphsen, and Christopher Nantista
Stanford Linear Accelerator Center, Menlo Park, 2575 Sand Hill Road, Menlo Park, California 94025, USA
(Received 29 October 2010; published 4 January 2011)

Acceleration gradient is a critical parameter for the design of future TeV-scale linear colliders. The major obstacle to higher gradient in room-temperature accelerators is rf breakdown, which is still a very mysterious phenomenon that depends on the geometry and material of the accelerator as well as the input power and operating frequency. Pulsed heating has been associated with breakdown for many years; however, there have been no experiments that clearly separate field and heating effects on the breakdown rate. Recently, such experiments have been performed at SLAC with both standing-wave and traveling-wave structures. These experiments have demonstrated that pulsed heating is limiting the gradient. Nevertheless the *X*-band structures breakdown studies show damage to the iris surfaces in locations of high electric field rather than of high magnetic field after thousands of breakdowns. It is not yet clear how the relative roles of electric field, magnetic field, and heating factor into the damage caused by rf breakdown. Thus, a dual-moded cavity has been designed to better study the electric field, magnetic field, and pulsed heating effects on breakdown damage.

DOI: 10.1103/PhysRevSTAB.14.010401 PACS numbers: 29.20.Ej, 52.59.−f, 84.40.Az

I. INTRODUCTION

The highest practical acceleration gradient achieved in a metal structure is about 10^8 V/m, far below the boundary material ionization gradient of about 10^{10} V/m. It is limited by material damage and rf breakdown in cavities as well as local surface field enhancement factor β. Two major reasons are thought to cause structure breakdown. First, the high electric field regions are tending to have explosive field emission, which could trigger breakdown [1,2]. From the high-power test results on the *X*-band single cell standing-wave (SW) structures and traveling-wave (TW) structures for JLC/NLC and CLIC, it indicates that the rf breakdown rate has a very strong dependence on electric field of $E_a{}^{30}$, where E_a donates the gradient at fixed pulse length [3]. However, recent experiments in an 18-cell *X*-band traveling-wave structure contradict this hypothesis. There the breakdown rate within the structure increased only linearly toward the downstream end despite the large (55%) increase in gradient [4]. Second, the high magnetic field regions are heating the surface up abruptly and inducing thermomechanical stress because of the nonuniform thermal expansion, known as pulsed heating effect. Such stress pulses may lead to fatigue deterioration of the surface [5,6]. The damaged surface will on the one hand worsen the surface conductivity thus increasing power losses, and on the other hand initiate crack propagation leading to failure. However, studies using single cell cavities [6,7] and multicell cavities [8] show damage to the surfaces on the irises in locations of high electric field instead of high magnetic field after thousands of breakdowns. It is still not clear how the electric field, magnetic field, and heating facts are affecting the breakdown.

Experimental results show that, from the comparison among the SW single cell cavities with various types of geometries [9–11] and the comparison of the waveguides with a low and high magnetic field [12], the breakdown is closely related to the pulsed heating. However, the effects of magnetic field and electric field are not separated from heating effects in these experiments. Recently, using rf pulses precisely shaped with a SLED-II pulse compressor, we have been able to distinguish field and heating effects in rf breakdown. The tests were done at *X* band on a single cell undamped SW cavity and a multicell damped TW cavity. The total pulses seen by the two cavities are about 10^8 and 2×10^8, respectively. All the experimental results are still repeatable with these cavities, which show that the cavities are not damaged by the cumulative breakdowns yet. This is the first clear demonstration that pulsed heating is limiting structure performance.

This paper is organized as follows. In Sec. II, the experimental results from an *X*-band (11.424 GHz) single cell SW cavity are presented, and in Sec. III, the results of a multicell *X*-band TW cavity are presented. A dual-moded cavity for future experiments is then described in Sec. IV. Finally, a discussion and summary is given in Sec. V.

II. EXPERIMENTAL RESULTS FROM AN *X*-BAND SINGLE CELL UNDAMPED SW CAVITY

Tests of an *X*-band single cell SW cavity were done in the next linear collider test accelerator at SLAC to take advantage of the rf stations there with SLED-II, which affords very high rf power (up to 200 MW with a 50 MW klystron). Figure 1 shows (a) a cutaway view of the cavity and (b) a TM_{01} mode launcher used to power the cavity axially to avoid field enhancing side-coupling

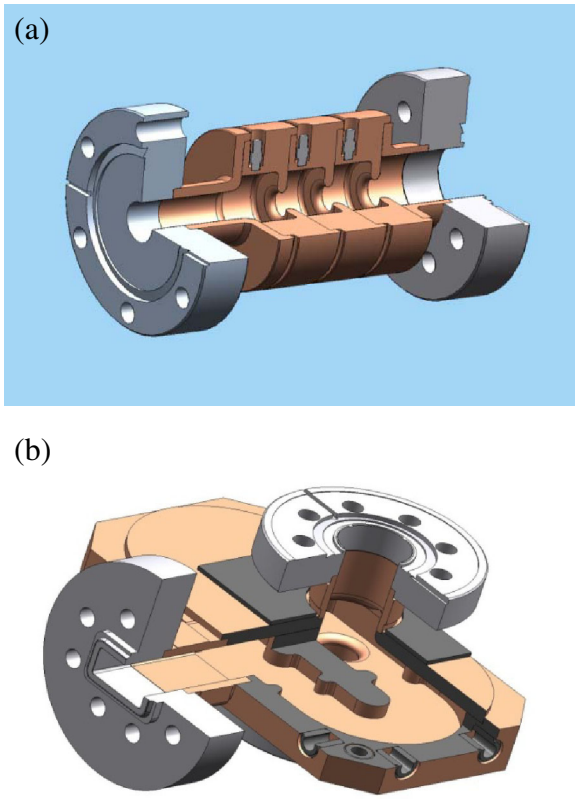

FIG. 1. Cutaway views of the "single cell" SW cavity (a) and the TM_{01} mode launcher (b).

apertures. The cavity is actually comprised of three cells operated in the π mode. However, as evident from the on-axis electric field bead pull plot in Fig. 2 [13], the middle cell should dominate breakdown events, since its field is by design about twice that in the others. Figure 3 is a picture of the high-power test setup for the cavity. The output power from SLED-II is divided by two 3 dB hybrids to the structure. A diagnostic cavity is installed downstream of the structure as a dark current monitor to record rf breakdowns.

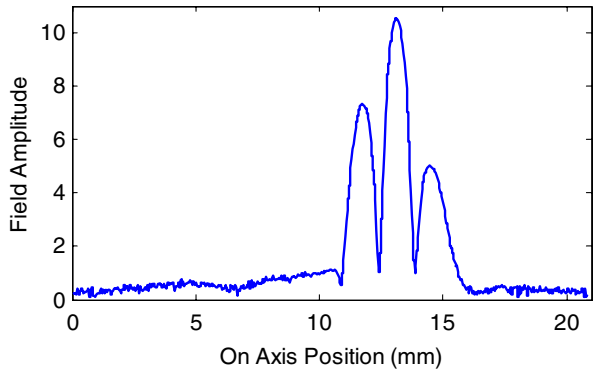

FIG. 2. The π-mode electric field profile along the cavity axis, from a bead pull before high-power testing.

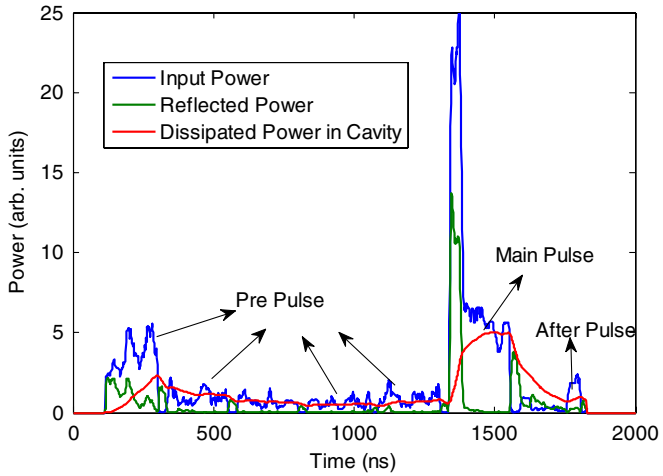

FIG. 3. The *X*-band SW single cell cavity high-power test setup.

By incorporating overshoot at the beginning of the compressed pulse, the effective cavity filling time can be shortened considerably. This is illustrated by Fig. 4, where the flat dissipated power during the rest of the main pulse indicates that steady state gradient for this input power has been roughly reached during the overshoot portion. By adjusting the phase in different time bins of the klystron pulse, as well as its overall amplitude, we can change the amount of rf in the part of the SLED-II output labeled prepulse while maintaining the same amplitude in the main pulse, as demonstrated in Fig. 5(a). This allows us to achieve different peak pulsed heating with a fixed main pulse and thus to distinguish between field and pulsed heating effects in rf breakdown.

Figure 5 shows waveforms and data plots from high-power operation of our single cell SW cavity with roughly the same main pulse duration and gradient but with

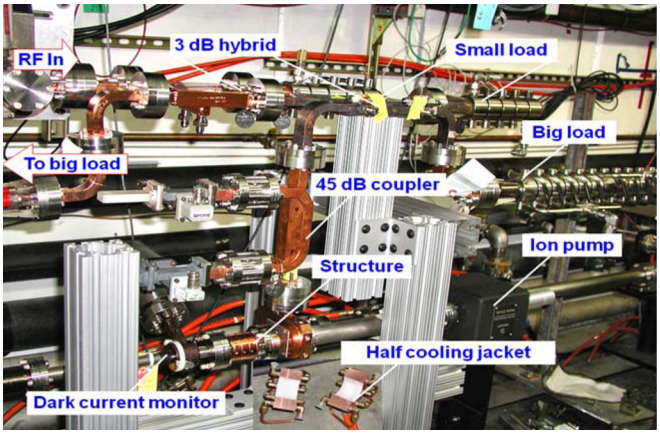

FIG. 4. The input forward, reflected, and dissipated power for the SW cavity test. The prepulse is the power leaked from SLED-II during compression, the main pulse is the discharged compressed pulse, and the after pulse is the remaining stored energy emitted from the delay lines after the klystron pulse.

different levels of peak pulsed heating, as deduced from the input forward and reflected power. The test results clearly show the breakdown rate is surely related to pulsed heating. Figure 6 illustrates a further experiment, in which near identical peak pulsed heating was produced during runs with different gradient during the main pulse. According to an established semiempirical mathematical relationship [3], the breakdown rate at 139 MV/m should be about

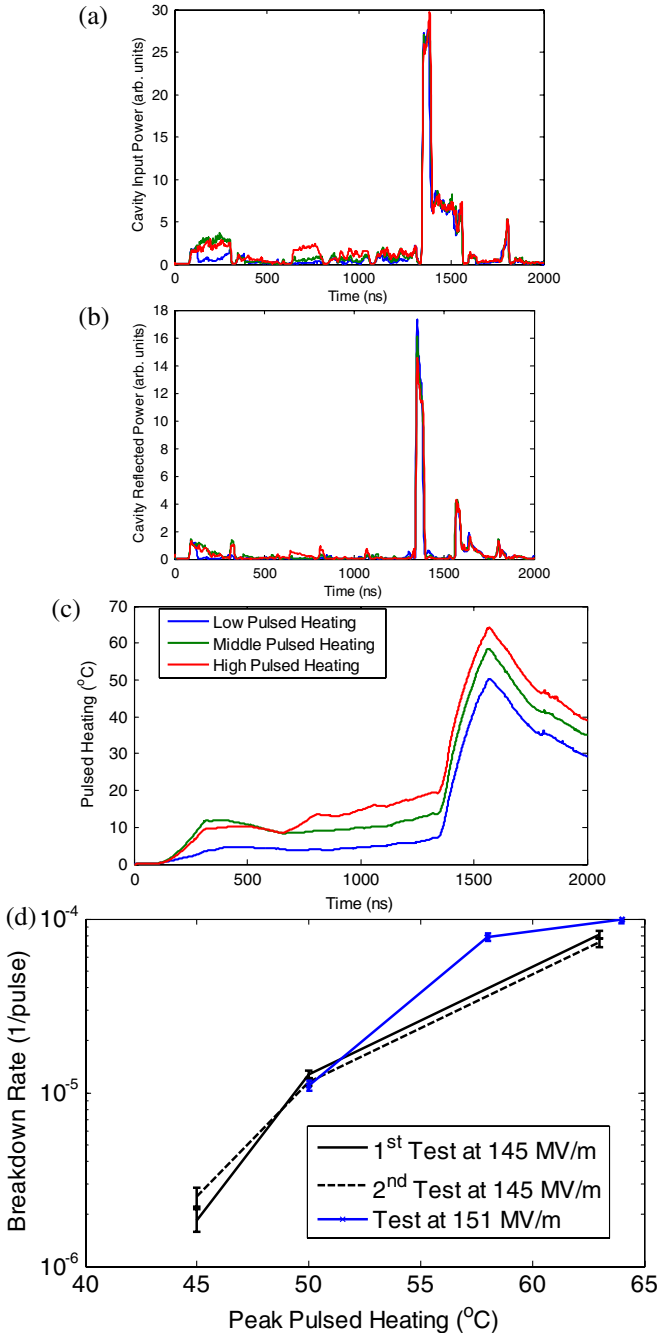

FIG. 5. (a) Input power waveforms, (b) corresponding reflected power, and (c) peak surface temperature rise profile for X-band single cell SW cavity test runs with similar main input pulses but different prepulses. (d) Test results.

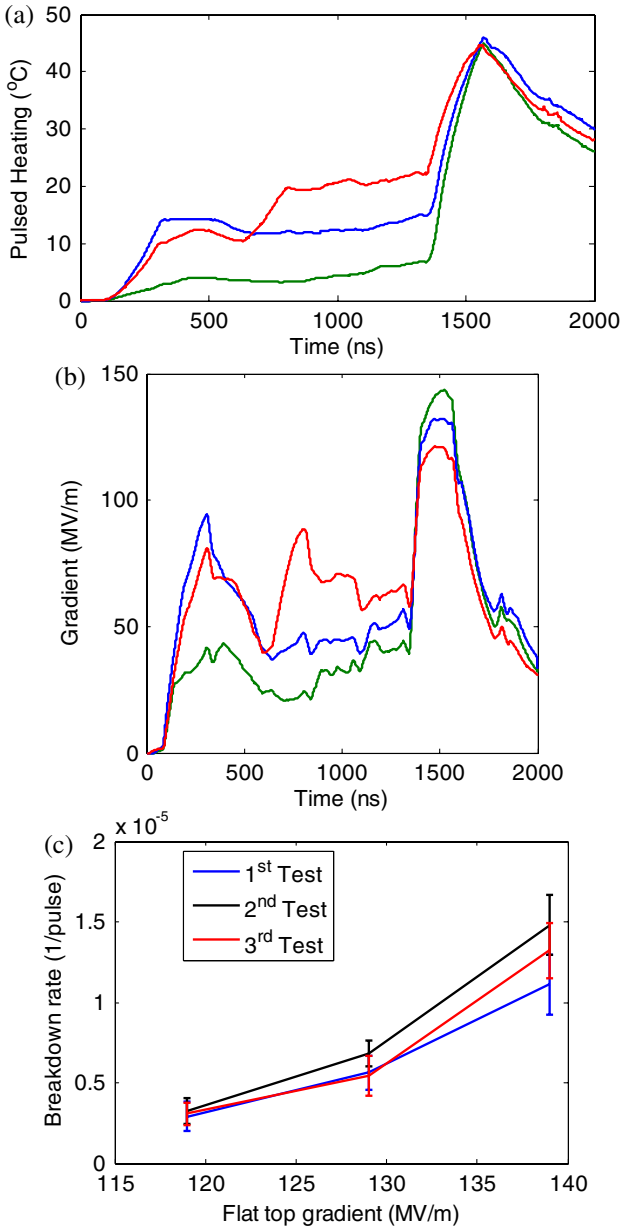

FIG. 6. (a) Peak surface temperature rise and (b) acceleration gradient profiles for X-band single cell SW cavity test runs with similar peak pulsed heating but different main pulse gradients. (c) Test results.

105 times what it is at 119 MV/m. The test results plotted in Fig. 6(c), however, only show a quadrupling of breakdown rate over this gradient range. According to these experiments, the breakdown rate varies depending on the pulsed heating temperature rise.

III. EXPERIMENT RESULTS FROM AN X-BAND DAMPED-CELL MULTICELL TW CAVITY

Figure 7 is a cutaway view of a cell of an X-band TW structure with coupling slots for damping of higher order modes. Unlike in a normal disk-loaded structure, the peak

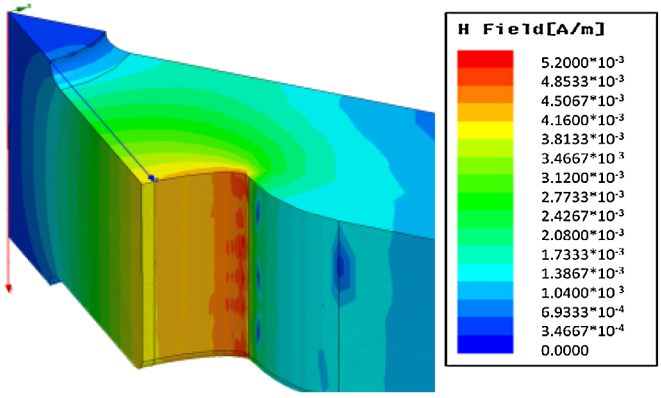

FIG. 7. Cutaway view of 1/8 of a cell of the multicell TW structure showing its surface magnetic field distribution.

pulsed heating is at the edge of the high order mode (HOM) coupling slot, not on the disk face [13]. The results of high-power breakdown tests at different gradients and pulse widths are plotted in Fig. 8, from which it is apparent that the breakdown rate is governed by the cavity peak pulsed heating.

Figure 9 shows power waveforms and plots of breakdown rate versus pulsed heating with and without preheating via rf power outside of the main compressed time bin. Also included in the plot is the result of achieving the higher heating by simply expanding the compressed pulse width. One can conclude that (1) breakdown rate is determined by pulsed heating for the same input main pulse, and (2) the same pulsed heating produces the same breakdown rate even when deposited with a different time structure.

These results contrast with those from *X*-band TW structures developed for the NLC program, in which the peak pulsed heating was about 20°C without HOM damping and doubled to 40°C with damping slots [14–16]. No systematic difference in the breakdown rates was observed between the damped and nondamped structures, whereas a nondamped version of the TW structure discussed here

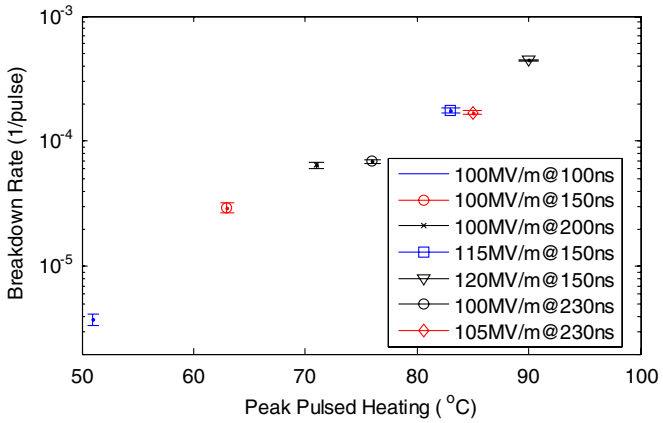

FIG. 8. The HOM-damped multicell *X*-band TW structure high-power test results.

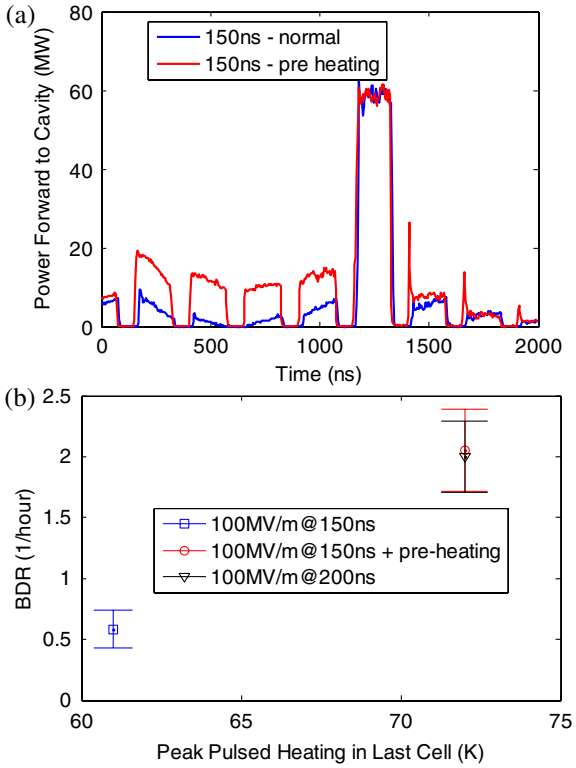

FIG. 9. (a) Input power waveforms and (b) test results for high-power runs of the HOM-damped multicell *X*-band TW cavity high-power test with and without prepulse heating.

performed much better (2 orders of magnitude lower breakdown rate for the same gradient and pulse width). Thus, we may surmise that the pulsed temperature rise needs to be above about 40–50°C for it to affect breakdown rate. In fact, it is above this level that one begins to observe surface damage caused by the repetitive stress induced by pulsed heating [5,16,17].

IV. A DUAL-MODED CAVITY

The above high-power test results on SW and TW cavities establish a clear relationship between pulsed heating and rf breakdown rate. However, it is still not clear how the combination of field (electric and magnetic) and pulsed heating affects breakdown. That is, the relative roles played by electric and magnetic surface fields in the phenomenon of rf breakdown are not completely understood.

TABLE I. Dual-moded cavity design parameters.

Parameter	TE_{011}	TEM_3
Q_0	15 162	9591
T_c $(= 2Q_L/\omega)$ (ns)	205	135
$\lvert E_s\rvert_p/\sqrt{P_{\rm in}}$ (kV/m/W$^{1/2}$)	19.62	110.2
$\lvert H_s\rvert_p/\sqrt{P_{\rm in}}$ (A/m/W$^{1/2}$)	233.6	302.4
$\lvert E_s\rvert_p/\lvert H_s\rvert_p$ (V/A)	84.0	3644

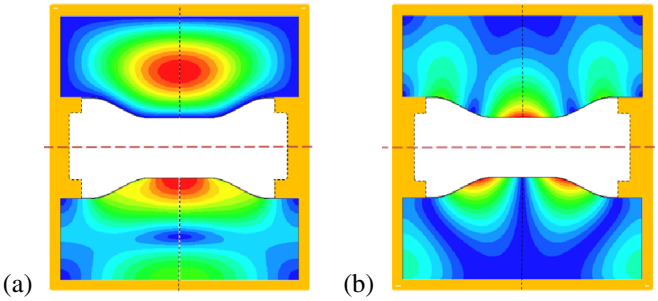

FIG. 10. Electric field pattern (top) and magnetic field pattern (bottom) for (a) the TE_{011} mode and (b) the TEM_3 mode in a coaxial rf breakdown test cavity with necked center conductor. The white region is a removable center conductor.

High magnetic fields, for example, have been known to cause surface melting in regions where no breakdowns occurred. Is it only through pulsed heating, i.e. the related surface currents, that magnetic field is relevant, or does the field itself play a role in the surface physics resulting in breakdown?

These questions cannot be easily addressed experimentally with a normal accelerator structure because the electric field and magnetic field are not independent. We present a design for a single, nonaccelerating, rf cavity resonant in two essentially degenerate modes, which, driven independently, allow the rf magnetic field to be increased on the region of highest electric field without affecting the latter. The design allows for the potential reuse of the cavity with different samples in the high-field region. The cavity is not itself of a geometry applicable to particle acceleration. However, it may provide information on the basic physics relevant to optimization of accelerator structure designs.

The design has been finalized, with simulations giving each mode within 0.2 MHz of 11.424 GHz and critically coupled to $0.96 < \beta < 1.04$. The edges of the coupling slots are rounded to 76 μm to reduce slot pulsed heating. Table I gives the quality factors, time constants, and steady state peak surface field amplitudes for each mode. The cavity field distribution for each mode is shown in Fig. 10. One mode produces a focused surface electric field maximum in a region where the other mode provides peak magnetic field, and thus pulsed heating. This region is on a center conductor in the modified coaxial geometry. The purpose of the design is to allow a series of rf breakdown experiments to be conducted with independent control of electric and magnetic field. The wall current patterns associated with the chosen modes permit breaks allowing the cavity to be opened at the midplane and the center conductor to be removed. Multiple experiments can thus be performed with the same cavity by simply replacing the center conductor.

V. SUMMARY

Various experiments have been performed over the past decade or so to investigate the physics of accelerating gradient limitation due to rf breakdown in normal conducting accelerator structures. Only recent experiments have conclusively demonstrated the strong correlation between pulsed heating and rf breakdown rate for cavities/structures with fairly high pulse heating. However, questions remain, such as why the breakdown damage in an accelerator is not where the peak pulsed heating is, and it is still not clear how the pulsed heating is limiting the performance of the structure. Hopefully, the coming high-power test of the dual-moded cavity will bring some useful information.

ACKNOWLEDGMENTS

We wish to thank Valery Dolgashev, James Lewandowski, Juwen Wang, Lisa Laurent, and the ARD Test Facilities Group for their efforts on the design, installation, cold testing, and high-power operation of the structures.

[1] J. W. Wang and G. A. Loew, Report No. SLAC-PUB-7684, 1997.
[2] G. A. Mesyats, *Explosive Electron Emission* (URO-Press, Ekaterinburg, 1998), pp. 218–222.
[3] A. Grudiev, S. Calatroni, and W. Wuensch, Phys. Rev. ST Accel. Beams **12**, 102001 (2009).
[4] C. Adolphsen *et al.*, Report No. SLAC-PUB-13697, 2009.
[5] D. P. Pritzkau and R. H. Siemann, Report No. SLAC-PUB-8554, 2000.
[6] Sami G. Tantawi, Report No. AAC2010, Annapolis, MD, 2010.
[7] L. Laurent, G. Garyotakis, and G. Scheitrum, Report No. SLAC-PUB-8409, 2000.
[8] W. Wuensch, in *Proceedings of the 8th European Particle Accelerator Conference, Paris, 2002* (EPS-IGA and CERN, Geneva, 2002).
[9] Roark A. Marsh, Ph.D. thesis, MIT, 2009.
[10] Valery Dolgashev *et al.*, in Proceedings of 1st International Particle Accelerator Conference: IPAC'10, Kyoto, Japan, 2010, THPEA060.
[11] V. A. Dolgashev, S. G. Tantawi, and C. D. Nantista, Report No. SLAC-PUB-12956.
[12] Valery A. Dolgashev and Sami G. Tantaw, in Proceedings of the 8th European Particle Accelerator Conference, Paris, 2002 (Ref. [8]).
[13] James Lewandowski (private communication).
[14] A. Grudiev (private communication).
[15] Valery A. Dolgashev, "Update on RF Pulsed Heating and Choke Accelerating Structures", 2002.
[16] C. Adolphsen, Report No. SLAC-PUB-9906, 2003.
[17] Z. Li *et al.*, Report No. SLAC-PUB-11916, 2006.